J Solid State Electrochem (2009) 13:1561–1566
DOI 10.1007/s10008-008-0730-0

ORIGINAL PAPER

Pt–Ru nanoparticles supported PAMAM dendrimer functionalized carbon nanofiber composite catalysts and their application to methanol oxidation

T. Maiyalagan

Received: 22 August 2008 / Revised: 6 October 2008 / Accepted: 4 November 2008 / Published online: 20 November 2008

Abstract Polyamidoamine (PAMAM) dendrimers has been anchored on functionalized carbon nanofibers (CNF) and supported Pt–Ru nanoparticles have been prepared with $NaBH_4$ as a reducing agent. The samples were characterized by X-ray diffraction, scanning electron microscopy, and transmission electron microscopy (TEM) analysis. It was shown that Pt–Ru particles with small average size (2.6 nm) were uniformly dispersed on PAMAM/CNF composite support and displayed the characteristic diffraction peaks of Pt face-centered cubic structure. The electrocatalytic activities of the prepared-composites (20% Pt–Ru/PAMAM-CNF) were examined by using cyclic voltammetry for oxidation of methanol. The electrocatalytic activity of the CNF-based composite (20% Pt–Ru/PAMAM-CNF) electrode for methanol oxidation showed better performance than that of commercially available Johnson Mathey 20% Pt–Ru/C catalyst. The results imply that CNF-based PAMAM composite electrodes are excellent potential candidates for application in direct methanol fuel cells.

Keywords Methanol oxidation · DMFC · Dendrimers · Nanostructured materials · Electro-catalyst

Introduction

Fuel cells operate with the electrochemical oxidation of hydrogen or methanol, as fuels at the anode and the reduction of oxygen at the cathode are attractive power sources due to their high conversion efficiencies, low pollution, light weight, and high power density. Methanol offers the advantage of easy storage and transportation when compared to hydrogen oxygen fuel cell, its energy density (~2,000 Wh/kg) and operating cell voltage (0.4 V) are lower than the theoretical energy density (~6,000 Wh/kg) and the thermodynamic potential (~1.2 V) [1, 2]. However, the fuel cells could not reach the stage of commercialization due to the high cost, which is mainly associated with the noble metal-loaded electrodes and the membrane. In order to reduce the amount of Pt loading on the electrodes, there have been considerable efforts to increase the dispersion of the metal on the support. The catalyst is very often found to disperse on a conventional carbon support, and the support material influences the catalytic activity through metal support interaction [3–5].

New novel carbon support materials such as graphite nanofibers (GNFs) [6, 7], carbon nanotubes (CNT) [8–12], carbon nanohorns [13], and carbon nanocoils [14] provide alternate candidates of carbon support for fuel cell applications. Bessel et al. [6] and Steigerwalt et al. [7] used GNFs as supports for Pt and Pt–Ru alloy electrocatalysts. They have observed better activity for methanol oxidation. The high electronic conductivity of GNF and the specific crystallographic orientation of the metal particles resulting from well-ordered GNF support are believed to be the factors for the observed enhanced electro-catalytic activity. In heterogeneous catalysis, one of the important tasks is the determination of the number of active sites in the catalyst. For a given catalyst, the number of active sites present is responsible for the observed catalytic activity. A considerable amount of research has been devoted toward understanding the number of active sites and the role played by the carrier of the supported catalysts. The most efficient utilization of any supported catalyst depends on

T. Maiyalagan (✉)
Department of Chemistry, School of Science and Humanities,
VIT University,
Vellore 632014, India
e-mail: maiyalagan@gmail.com

the percentage of exposed or the dispersion of the active component on the surface of the carrier material. Among the various factors that influence the dispersion of an active component, the nature of the support and the extent of the active component loading are of considerable importance.

Without surface modification, most of the carbon nanomaterials lack sufficient binding sites for anchoring precursor metal ions or metal nanoparticles, which usually lead to poor dispersion and the aggregation of metal nanoparticles, especially at high loading conditions. To introduce more binding sites and surface anchoring groups, an acid oxidation process was very frequently adopted to treat carbon nanomaterials in a mixed acid aqueous solution, which introduces surface bound polar hydroxyl and carboxylic acid groups for subsequent anchoring and reductive conversion of precursor metal ions to metal nanoparticles [15].

Generally, metal nano-particles have been synthesized for the purpose of increasing the catalytic surface area in comparison to bulk metal and have utilized strategies such as stabilization in a soluble polymer matrix or encapsulation in dendrimers to protect them from aggregation. Dendrimers are good candidates for preparing metal nanoparticles because they can act as structurally and well-defined templates and robust stabilizers. Polyamidoamine (PAMAM) dendrimers, in particular, have been used as nanoreactors with effective nanoparticle stabilization. In addition, encapsulated nanoparticles surfaces are accessible to substrates so that catalytic reactions can be carried out [16–18].

PAMAM dendrimer encapsulated Pt nanoparticles and PtPd bimetallic nanoaparticles are electrocatalytically active for oxygen reduction [19–21]. Also dendrimer-encapsulated platinum nanoparticles supported on carbon fiber and nitrogen-doped CNT as electrodes for oxygen reduction [22, 23].

In addition, platinum–ruthenium alloys are the best catalysts for methanol oxidation direct methanol fuel cells [24, 25]. PAMAM dendrimers were modified with a Ni-cyclam as novel electrocatalytic material for the electrochemical oxidation of methanol [26]. Kim et al. [27] have reported the preparation of platinum–dendrimer hybrid nanowires using alumina templates, which exhibited and enhanced electro-catalytic activity toward methanol oxidation. PAMAM dendrimer (PAMAM 4.5)-encapsulated Pt nanoparticles chemically linked to gold substrates through a cystamine monolayer exhibited electrocatalytic activity toward the oxidation of methanol [28].The terminal functional groups of the dendrimers stabilizes metal nanoparticles without aggregation. In this paper, we make use of the fourth-generation amine-terminated PAMAM dendrimers (G_4-NH_2) to anchor on the functionalized carbon nanofiber (CNF) as a substrate and then encapsulate Pt–Ru nanoparticles on dendrimers for the better dispersion of the electrode, which exhibited very good catalytic activity. These materials are characterized and studied, using X-ray diffraction (XRD), scanning electron microscopy (SEM), transmission electron microscopy (TEM), and cyclic voltammetry. The electrochemical properties of the composite electrode (Pt–Ru–PAMAM/CNF) were compared to those of the commercial electrode (Pt–Ru/C), using cyclic voltammetry. The 20% Pt–Ru–PAMAM/CNF exhibited excellent catalytic activity and stability when compared to the 20 wt.% Pt–Ru/C.

Experimental

Materials

All the chemicals used are of analytical grade. CNFs (grade PR 24 LHT) are commercially available from Pyrograf, USA. 1-(3-Dimethyl-aminopropyl)-3-ethyl-carbodiimide-hydrochloride (EDC), *N*-hydroxysuccinimide (NHS), hexachloroplatinic acid, and ruthenium (III) chloride hydrate are procured from Sigma-Aldrich and used as received. Vulcan XC-72 carbon black is purchased from Cabot. Methanol and sulfuric acid are obtained from Fischer Chemicals. Nafion 5 wt.% solution is obtained from Dupont and is used as received. Fourth generation amine-terminated polyamidoamine PAMAM dendrimers (G4-NH_2) with the highest available purity (10 wt.% in methanol) are obtained from Aldrich and used without further purification.

Functionalization of CNF

The CNF is treated with mixed acid aqueous solution of HNO_3 and H_2SO_4 in 1:3 ratios under magnetic stirrer for 3 h. It is then washed with water and evaporated to dryness.

Preparation of CNF-PAMAM

Fifty milliliters of 0.1 mg/ml carboxylated CNF containing 100 mg of EDC and 100 mg of NHS is slowly added into a methanol solution of 20% G4 PAMAM under high speed agitating.

Preparation of Pt–Ru–PAMAM/CNF catalysts:

6.15 mM H_2PtCl_6 and 11.8mM $RuCl_3$ and dendrimer encapsulated CNF are mixed by keeping the solution under magnetic stirrer for 3 h. Five milliliters of 0.1 M $NaBH_4$ is added to the solution and kept under evaporation. A schematic of the detailed procedure for the electrocatalyst preparation is shown in Fig. 1.

Characterization

The phases and lattice parameters of the catalyst are characterized by XRD patterns employing Shimadzu XD-

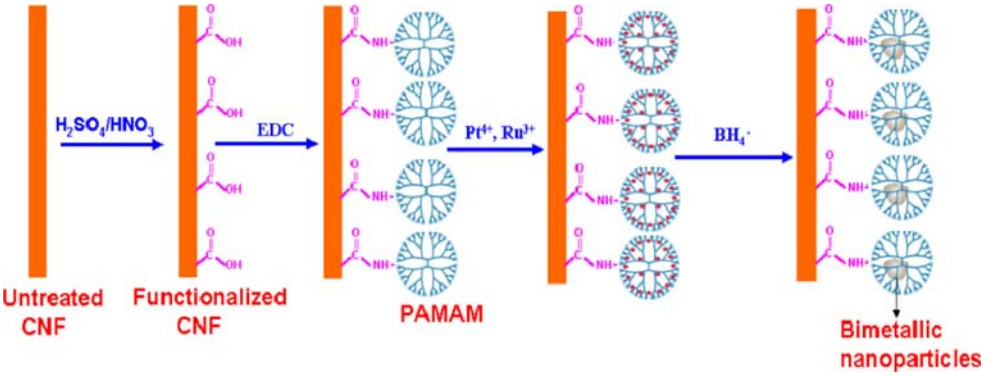

Fig. 1 Schematic diagram illustrating synthesis of Pt–Ru–PAMAM/CNF

D1 diffractometer using Cu K_α radiation (λ=1.5418 Å) operating at 40 kV and 48 mA. XRD samples are obtained by depositing composite supported nanoparticles on a glass slide and drying the latter in a vacuum overnight. The scanning electron micrographs are obtained using JEOL JSM-840 model, working at 15 keV. For TEM studies, the composite dispersed in ethanol are placed on the copper grid, and the images are obtained using JEOL JEM-3010 model, operating at 300 keV.

Electrochemical measurements

All electrochemical measurements are performed using a BAS Epsilon potentiostat. A three-electrode cell is used, which consisted of the glassy carbon (0.07 cm^2) as working electrode and Pt foil and Ag/AgCl (saturated by KCl solution) electrodes as counter and reference electrodes, respectively, are used. All the electrochemical experiments are carried out at room temperature in 0.5 M H_2SO_4 electrolyte. The electrolyte solution is purged with high pure nitrogen for 30 min prior to a series of voltammetric experiments.

Preparation of the working electrode

Glassy carbon (GC) (Bas Electrode, 0.07 cm^2) is polished to a mirror finish with 0.05 μm alumina suspensions before each experiment and served as an underlying substrate of the working electrode. In order to prepare the composite electrode, the catalysts are dispersed ultrasonically in water at a concentration of 1 mg ml^{-1} and 20-μl aliquot is transferred on to a polished GC substrate. After the evaporation of water, the resulting thin catalyst film is covered with 5 wt.% Nafion solution. Then, the electrode is dried at 353 K and used as the working electrode. A solution of 1 M CH_3OH in 0.5 M H_2SO_4 is used to study the methanol oxidation activity.

Result and discussion

The crystal structures of the catalysts are examined by XRD as shown in Fig. 2. Characteristic reflections of Pt face-centered cubic structure can be observed. X-ray scattering from the CNF support is evidenced by the peak at 26° in 2θ. The diffraction peaks of the catalyst (Pt–Ru/C) are observed to be sharp with a high intensity indicating high crystallinity (Fig. 2a). On the contrary, very broad peaks with weak intensity are observed for PAMAM containing composites (Pt–Ru/PAMAM-CNF), indicating that they are not fully crystalline in nature (Fig. 2 b) as observed for the commercial Pt–Ru/C (JM) (Fig. 2a). Compared with Pt–Ru/C, the peak intensities of Pt–RuPt–PAMAM/CNF are lower and the full width at half-maximum (FWHM) for the peaks are bigger. Bigger FWHM indicates a smaller average size of metal nanoparticles on PAMAM/CNF composite. No evidence of peaks related to Ru was found in these catalysts. The absence of diffraction peaks typical for Ru can be due to a number of reasons such as Ru not being dissolved in the Pt lattice, that is, forming a PtRu alloy and/or the Ru being present in the amorphous form, as further discussed below [29, 30]. The position of the Pt (111) peak for the larger (>1.2 nm) sized catalysts is shifted

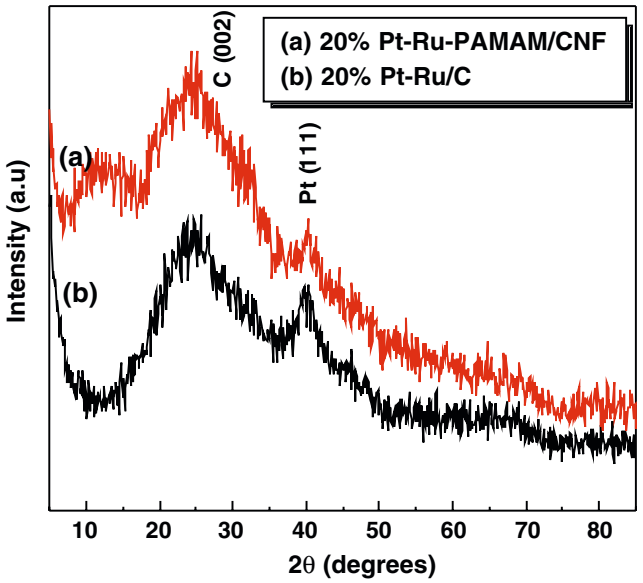

Fig. 2 XRD spectra of **a** Pt–Ru/C, **b** Pt–Ru–PAMAM/CNF

to higher 2θ positions than that for pure Pt that has a maxima at 39.7645° [31].

The scanning electron micrograph images of commercial CNFs are shown in Fig. 3a,b. The diameter of the nanofibers is measured using a Leica Qwin Image Analyzer and is found to be in the range of 260–250 nm and the length of about 100 μm. Figure 3c shows the image of Pt–Ru–PAMAM/CNF. According to the EDX measurements (Fig. 4), catalysts prepared in this work contained 20.1 wt.% of total metal with a Pt/Ru atomic ratio of 1:1.0~1.1, which agrees well with the stoichiometric ratio of 1:1 used in the starting mixture.

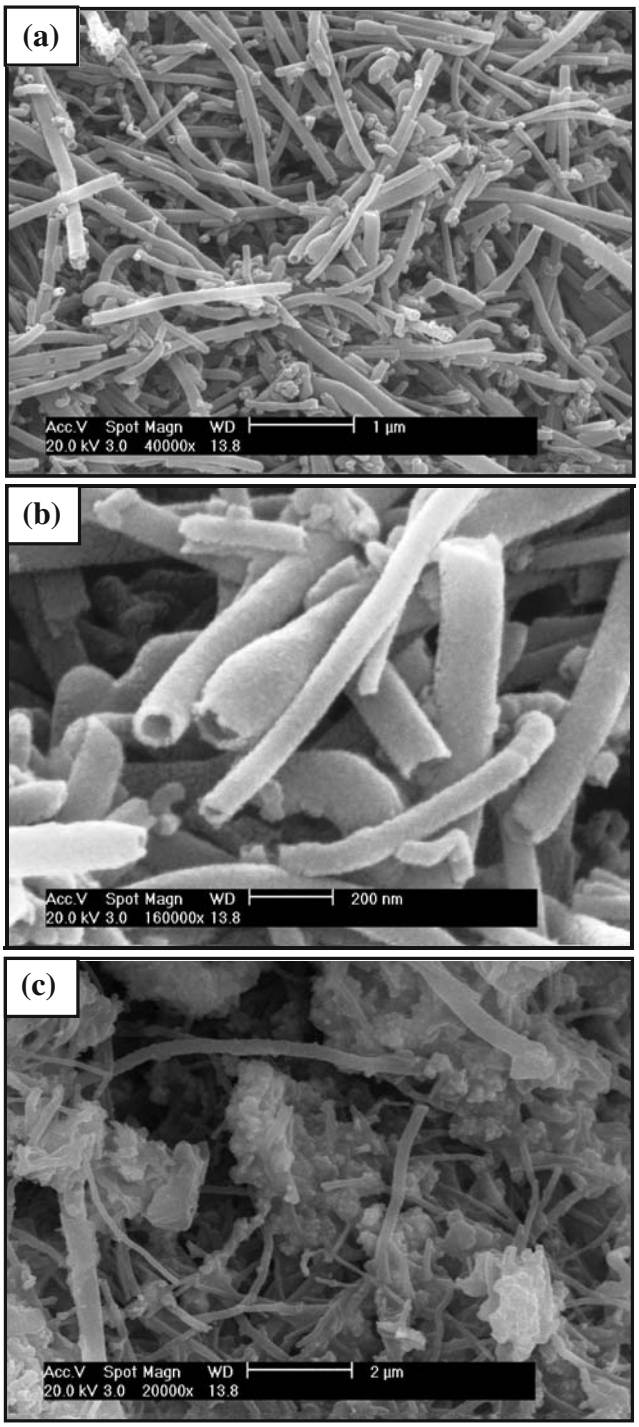

Fig. 3 SEM images of **a**, **b** CNF and **c** Pt–Ru–PAMAM/CNF

The TEM image of the prepared Pt–Ru–PAMAM/CNF catalysts, shown in Fig. 5, reveals that well-dispersed, spherical particles were anchored onto the external walls of PAMAM/CNF composite support with an average size of 2.6 nm. There is no agglomeration of Pt–Ru nanoparticles in the composite, and the Pt–Ru nanoparticles were found to be uniformly dispersed. In comparison, a commercial Johnson Matthey Pt–Ru catalyst (20 wt.% on Vulcan) had an average particle size of 3 nm. The uniform dispersion of metal nanoparticles on PAMAM/CNF composite is clearly due to the PAMAM dendrimer, which offers large and uniform distributed nitrogen-active sites for anchoring metal ions and metal nanoparticles. In this regard, PAMAM-functionalized CNF composite are far more effective supports than the conventional-acid-oxidized CNF. The conventional-acid oxidation functionalization leads to the structural damage of CNF, which causes a large extent of loss in electrical conductivity and thus potentially reduces the electrocatalytic activity of the catalyst. The three-dimensional structure, smaller particle size, and high dispersion of nanoparticles may result in large valuable Pt surface area and good electrocatalytic properties toward methanol oxidation.

The electrocatalytic activities for methanol oxidation of Pt–Ru–PAMAM/CNF and commercial Pt–Ru/C electrocatalysts are analyzed by cyclic voltammetry in an electrolyte of 0.5 M H_2SO_4 and 1 M CH_3OH at 50 mV/s. Figure 6 shows the cyclic voltammograms (CVs) of the synthesized Pt–Ru–PAMAM/CNF and commercial Pt–Ru/C catalysts in an electrolyte solution of 0.5 M H_2SO_4 and 1 M CH_3OH. There are two irreversible current peak during the

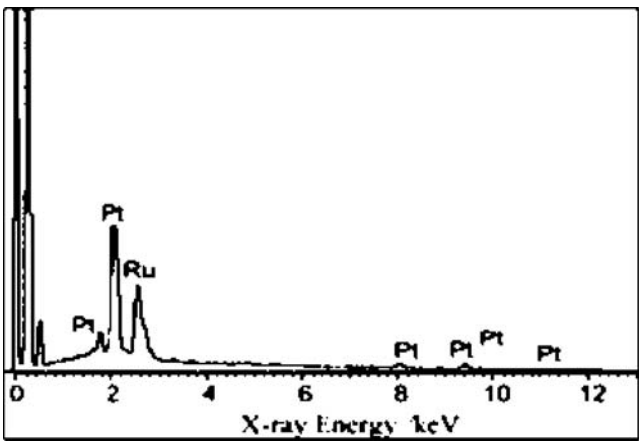

Fig. 4 EDX spectrum of Pt–Ru–PAMAM/CNF (PtRu 20.1 wt. %; Pt/Ru=1:1.0~1.1)

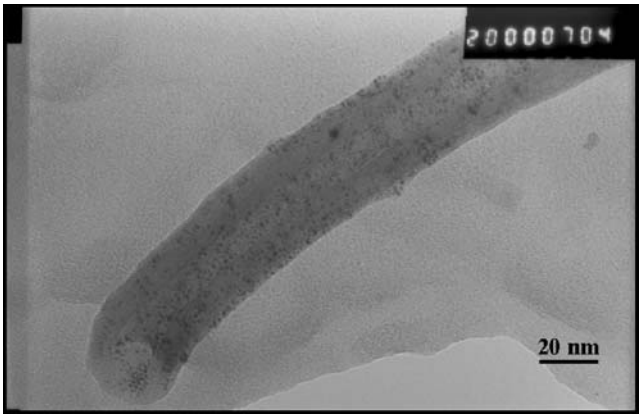

Fig. 5 TEM image of 20% Pt–Ru–PAMAM/CNF catalyst

electro-oxidation of methanol that are typically attributed on the forward scan peak at around 0.8 V to methanol electro-oxidation and on the backward peak at 0.6 V to the faradic oxidation reaction on the Pt of the residual intermediate species. Both CV curves reveal a similar shape and peak position, which is also in good agreement with previous reports for methanol CVs over supported Pt catalysts. The Pt–Ru–PAMAM/CNF composite shows higher electrocatalytic activity of methanol oxidation compared to Pt–Ru/C (JM) catalyst. The enhanced catalytic activity of Pt–Ru/PAMAM–CNF composite catalyst is due to higher dispersion of Pt–Ru nanoparticles and may be better oxidation of CO intermediates during methanol oxidation [32, 33].

The ratio of the forward anodic peak current (I_f) to the reverse anodic peak current (I_b) can be used to describe the catalyst tolerance to accumulation of carbonaceous species [34–38]. A higher ratio indicates more effective removal of the poisoning species on the catalyst surface. The I_f/I_b ratios of Pt–Ru–PAMAM/CNF and Pt–Ru/C are 1.36 and 0.87, respectively, showing better catalyst tolerance of PAMAM/CNF composites. There is no much decrease in electrocatalytic activity of the Pt–Ru–PAMAM/CNF composite catalysts on subsequent cycles of methanol oxidation compared to the Pt–Ru/C catalysts. This not only demonstrates the reproducibility of the results but also the stability of the nanoparticles on the PAMAM/CNF composite catalysts.

Similarly, Fig. 7 shows the chronoamperometric studies of the synthesized sample, which reveals the stability of the Pt–Ru–PAMAM/CNF catalyst toward the methanol electro-oxidation. The results are consistent with the view that PAMAM is not only stabilizing the Pt–Ru nanoparticles but is also enhancing the methanol oxidation currents under chronoamperometric conditions. Pt–Ru nanoparticles are well stabilized by amine-terminated PAMAM dendrimers. The high electrocatalytic activity of the Pt–Ru–PAMAM/CNF composite electrodes prepared in this work is most probably due to the very high dispersion of PtRu particles and the extensive presence of RuO*x*H*y*.

Conclusions

In summary, well-dispersed Pt–Ru nanoparticles have been synthesized on PAMAM–CNFs composite. The choice of the PAMAM G4-NH_2 dendrimer template and terminal amine functional groups provides for uniform preparation of size monodisperse catalysts and facilitates the controlled dispersion. The enhancements in activity and stability over Pt–Ru/PAMAM–CNF catalyst have been solely attributed to high dispersion Pt–Ru nanoparticles on the composite.

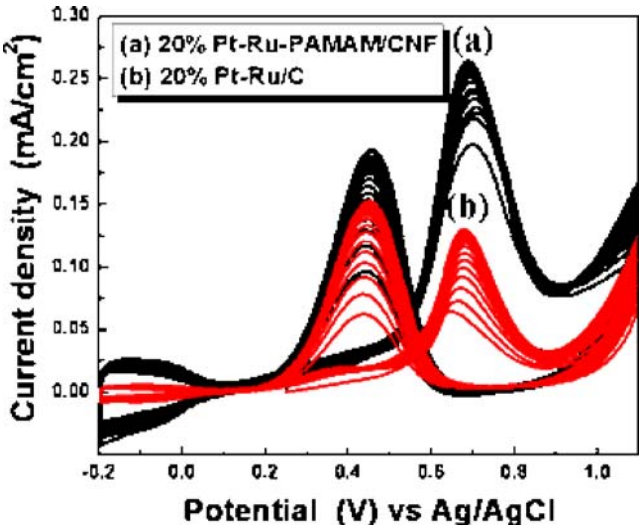

Fig. 6 Cyclic voltammogram of **a** Pt–Ru–PAMAM/CNF and **b** Pt–Ru/C in electrolyte solution of 0.5 M H_2SO_4 with 1 M CH_3OH at a sweep rate of 50 mV/S at room temperature

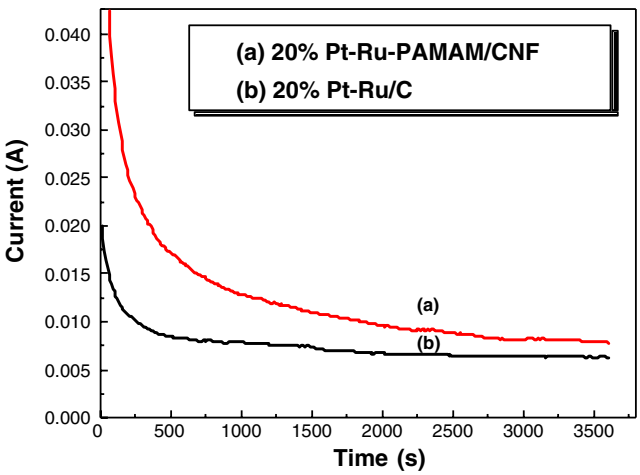

Fig. 7 Chronoamperometry of **a** Pt–Ru–PAMAM/CNF, **b** Pt–Ru/C polarized at +0.6 V in 0.5 M H_2SO_4/1 M CH_3OH

These findings suggest that Pt–Ru–PAMAM/CNF should be considered a good electrocatalyst material for direct methanol fuel cells. Though more work is needed to understand the fundamentals of the interaction between metal nanoparticles and dendrimers, particularly Pt–Ru–PAMAM/CNF, they show a potential as new electrocatalysts for low temperature fuel cells.

References

1. McNicol BD, Rand DAJ, Williams KR (2001) J Power Sources 83:47 doi:10.1016/S0378-7753(01)00882-5
2. Carrette L, Friedrich KA, Stimming U (2001) Fuel Cells (Weinh) 1:5 doi:10.1002/1615-6854(200105)1:1<5::AID-FUCE5>3.0.CO;2-G
3. Uchida M, Aoyama Y, Tanabe N, Yanagihara N, Eda N, Ohta A (1995) J Electrochem Soc 142:2572 doi:10.1149/1.2050055
4. Antolini E (2007) Appl Catal B Enviromental 724:324 doi:10.1016/j.apcatb.2007.03.002
5. Matsumoto T, Komatsu T, Arai K, Yamazaki T, Kijima M, Shimizu H, Takasawa Y, Nakamura J (2004) Chem Commun 7:840 doi:10.1039/b400607k
6. Bessel CA, Laubernds K, Rodriguez NM, Baker RTK (2001) J Phys Chem B 105:1115 doi:10.1021/jp003280d
7. Steigerwalt ES, Deluga GA, Lukehart CM (2002) J Phys Chem B 106:760 doi:10.1021/jp012707t
8. Li WZ, Liang CH, Zhou WJ, Xin Q (2003) J Phys Chem B 107:6292 doi:10.1021/jp022505c
9. Kim C, Kim YJ, Kim YA, Yanagisawam T, Park KC, Endo M, Dresselhaus MS (2004) J Appl Phys 96:5903 doi:10.1063/1.1804242
10. Wang C, Waje M, Wang X, Tang JM, Haddon RC, Yan YS (2004) Nano Lett 4:345 doi:10.1021/nl034952p
11. Maiyalagan T (2008) Appl Catal B Enviromental 89:286 doi:10.1016/j.apcatb.2007.11.033
12. Maiyalagan T, Viswanathan B, Varadaraju UV (2005) Electrochem Commun 7:905 doi:10.1016/j.elecom.2005.07.007
13. Yoshitake T, Shimakawa Y, Kuroshima S, Kimura H, Ichihashi T, Kubo Y (2002) Physica B 323:124 doi:10.1016/S0921-4526(02)00871-2
14. Hyeon T, Han S, Sung YE, Park KW, Kim YW (2003) Angew Chem Int Ed 42:4352 doi:10.1002/anie.200250856
15. Yu RQ, Chen LW, Liu QP (1998) Chem Mater 10:718 doi:10.1021/cm970364z
16. Knecht MR, Wright DW (2004) Chem Mater 16:4890 doi:10.1021/cm049058t
17. Zhao MQ, Crooks RM (1999) Adv Mater 11:217 doi:10.1002/(SICI)1521-4095(199903)11:3<217::AID-ADMA217>3.0.CO;2-7
18. Zhao MQ, Crooks RM (1999) Chem Mater 11:3379 doi:10.1021/cm990435p
19. Ye H, Crooks RM (2005) J Am Chem Soc 127:4930 doi:10.1021/ja0435900
20. Zhao M, Crooks RM (1999) Adv Mater 11:217 doi:10.1002/(SICI)1521-4095(199903)11:3<217::AID-ADMA217>3.0.CO;2-7
21. Ye H, Crooks RM (2007) J Am Chem Soc 129:3627
22. Ledesma-Garci J, Escalante Garci IL, Rodri FJ, Chapman TW, Godinez LA (2008) J Appl Electrochem 38:515 doi:10.1007/s10800-007-9466-2
23. Vijayaraghavan G, Stevenson KJ (2007) Langmuir 23:5279 doi:10.1021/la0637263
24. Wasmus S, Küver A (1999) J Electroanal Chem 461:14 doi:10.1016/S0022-0728(98)00197-1
25. Gasteiger HA, Markovic N, Ross PN, Cairns EJ (1994) J Phys Chem 98:617 doi:10.1021/j100053a042
26. Gonzalez-Fuentes MA, Manrıquez J, Gutierrez-Granados S, Alatorre-Ordaz A, Godınez LA (2005) Chem Commun 8:898 doi:10.1039/b412442a
27. Kim JW, Choi E-A, Park S-M (2003) J Electrochem Soc 150: E202 doi:10.1149/1.1554727
28. Raghu S, Nirmal RG, Mathiyarasu J, Berchmans S, Phani KLN, Yegnaraman V (2007) Catal Lett 119:40 doi:10.1007/s10562-007-9154-1
29. Wang DL, Zhuang L, Lu JT (2007) J Phys Chem C 111:16416 doi:10.1021/jp073062l
30. Guo JS, Sun GQ, Sun SG, Yan SY, Yang WQ, Qi J, Yan YS, Xin Q (2007) J Power Sources 168:299 doi:10.1016/j.jpowsour.2007.02.085
31. Bock C, Paquet C, Couillard M, Botton GA, MacDougall B (2004) J Am Chem Soc 126:8028 doi:10.1021/ja0495819
32. Jarvi TD, Stuve EM (1998) In: Lipkowski J, Ross PN (eds) Electrocatalysis, frontiers of electrochemistry series, Chapter 3. Wiley-VCH, New York, pp 75–153
33. Mukerjee S, McBreen J (1998) J Electroanal Chem 448:163 doi:10.1016/S0022-0728(97)00018-1
34. Mu Y, Liang H, Hu J, Jiang L, Wan L (2005) J Phys Chem B 109:22212 doi:10.1021/jp0555448
35. Manoharan R, Goodenough JB (1992) J Mater Chem 2:875 doi:10.1039/jm9920200875
36. Liu Z, Ling XY, Su X, Lee JY (2004) J Phys Chem B 108:8234 doi:10.1021/jp049422b
37. Deivaraj TC, Lee JY (2005) J Power Sources 142:43 doi:10.1016/j.jpowsour.2004.10.010
38. Maiyalagan T, Nawaz Khan F (2008) J Nanosci Nanotechnol doi:10.1016/j.catcom.2008.10.011